

<sup>1</sup>Banothu.Balasubramanyam  
<sup>2</sup>Balasubbareddy Mallala  
<sup>3</sup>G.Mallesham

## A fuzzy integrated non-linear backstepping control of a grid connected PMSG wind farm



**Abstract:** - In this paper a grid connected PMSG wind farm is controlled by non-linear backstepping control. The PMSG power is delivered to grid through two back-to-back connected IGBT based VSCs. The VSCs are controlled by individual Sin PWM techniques for which the reference signals are generated non-linear backstepping controller. A capacitor is connected at the common DC link of the back-to-back VSCs for voltage stability. The backstepping controller designed for the control of PMSG has the capability to extract maximum power from the wind farm. The machine side connected VSC operates in synchronization to the rotor angle and the grid side connected VSC operates in synchronization with the grid voltages. The DC voltage regulator of the grid side converter control should be optimum for better stability of the system. Therefore, the conventional PI controller of the voltage regulator is replaced by a 49-rule base FLC which reduces the ripple and settling time of the DC link voltage. A 2MG PMSG wind farm is considered for performance analysis with PI and FLC in the non-linear backstepping control structure. The comparative analysis is carried out in MATLAB software with Simulink block sets utilized to design the wind farm connected to grid. The graphs are compared to determine the performance of the controller with different operating conditions.

**Keywords:** PMSG (Permanent Magnet Synchronous Generator), IGBT (Insulated Gate Bipolar Transistor), VSC (Voltage Source Converter), PWM (Pulse Width Modulation), PI (Proportional Integral), FLC (Fuzzy Logic Controller), MATLAB Simulink.

### I. INTRODUCTION

With the increase in population the electrical power demand is also increasing day by day throughout the world. To meet the demand, fossil fuel power generation is no more a viable option. As the fossil fuel power plants are one of the causes of global warming and natural calamities. These fossil fuel plants need to be replaced by renewable power generation plants which generate power from natural resources [1]. From past few years researches on renewable sources are in rapid increase to create sustainable green energy with no carbon emissions. Solar power plants and wind farms are considered to be most promising renewable sources. Due to abundant availability of solar irradiation and winds, these sources are considered as never depleting natural sources. Wind farms comparatively generate more power than the solar plants for a given area of location. The efficiency of wind farms is considerably very high compared to solar plants. The only drawback of the wind farms is it cannot be installed in residential or human interference locations. The wind farms can only be installed at locations far away from people habitat places as they can be disastrous living nearby.

There are majorly two types of wind farms, offshore and onshore wind farms [2]. The offshore wind farms are considered to be more efficient and consistent power generation units because of installation in seas. The onshore wind farms are installed on land which have variable wind speeds and also at lower range of 5m/s to 12m/s. Therefore, more efficient machines, converters and controllers need to be adopted for the onshore wind farms. The PMSG is considered to be more efficient and low maintenance machine as the rotor is a permanent magnet [3]. Due to the permanent magnet rotor, external excitation circuit can be avoided reducing the cost and space of utilization. Compact wind farms can be fabricated with the used of PMSG machines. However, the limitation of the PMSG machine is that the voltage output drastically varies with change in wind speeds [4]. To avoid unsynchronized voltage sharing with the grid the PMSG is connected to a two-stage conversion system.

The first stage is the rectification stage which converts the variable AC voltages of the PMSG to DC voltage. The DC voltage is stabilized by the controller operating the rectifier by taking feedback from machine parameters [5]. The second stage is the inverting stage where the stabilized DC voltage is converted to AC voltages for sharing to the grid. The inverter is operated in synchronization to the grid voltages to ensure sharing of wind power to the grid. The complete structure of the PMSG wind farm involves a back-to-back connected 6-switch VSCs with a capacitor ( $C_{dc}$ ) at the DC link. The circuit structure of the PMSG wind farm can be observed in figure 1.

<sup>1</sup> \*Corresponding author: Department of Electrical Engineering, Osmania University, Hyderabad, Telangana State, India

<sup>2</sup> Department of Electrical & Electronics Engineering, Chaitanya Bharathi Institute of Technology, Hyderabad, Telangana State, India

<sup>3</sup> Department of Electrical Engineering, Osmania university, Hyderabad, Telangana State, India

Copyright © JES 2024 on-line : journal.esrgroups.org

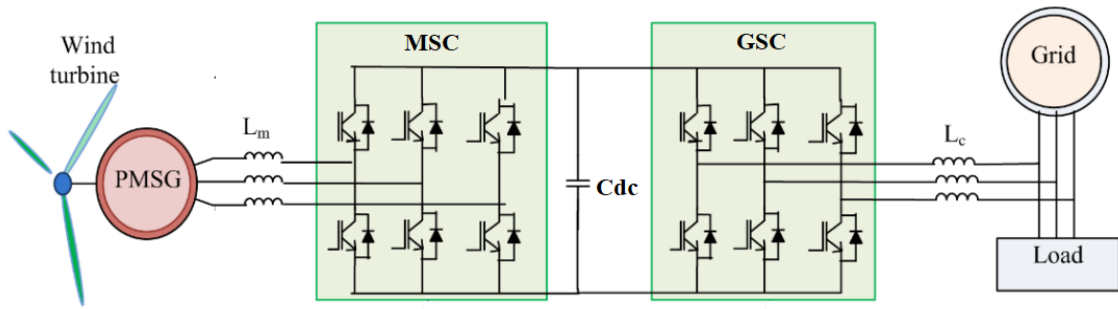


Figure 1: Circuit structure of PMSG wind farm

Both the MSC (Machine Side Converter) and GSC (Grid Side Converter) are controlled by individual non-linear backstepping controllers [6]. The MSC is operated as per the rotor speed and rotor angle of PMSG and the GSC is operated as per the 3-ph grid voltages. All the IGBTs of the back-to-back connected VSCs are controlled by Sin PWM technique receiving references signals from non-linear backstepping controllers. The GSC controller DC voltage regulator is updated with FLC which is designed with 49-rule base for high resolution control [7]. With more membership functions in FLC the value generation can be controlled creating stable and fast responding signals for the controller. With faster response of the controller the stabilization of the system also happens faster. As the FLC is introduced at the DC voltage regulator the DC link voltage stability and settling time improves. A comparative analysis is carried on the PMSG wind farm system with conventional PI and novel FLC non-linear backstepping controllers.

The paper is arranged with introduction of the PMSG wind farm test system in section 1 followed by section 2 which includes Backstepping control design for the MSC and GSC modules. The section 3 has the design and modeling of the FLC module for the GSC update using Fuzzy tool of MATLAB software. The simulation analysis of the proposed system is performed and the results are presented in section 4 including parameter graphs. The final section 5 is the conclusion to the paper finalizing the better control module for the PMSG wind farm determined by the results generated by the simulation analysis.

## II. BACKSTEPPING CONTROL DESIGN

Extracting power from renewable sources at stable voltages even during variable power generation is a critical task. This can be achieved by controlling the power electronic converting circuits with advanced controls structures [8]. The conventional methods involve only simple modulation technique with feedback from grid and machine. These methods have faster response but also have very less stability to the variations occurring on the system. As the disturbances are high the oscillations will be more and the controller is more prone to fail. In this paper a non-linear backstepping control structures for MSC and GSC are designed for stable operation of the PMSG wind farm. The MSC is controlled as per the rotor angle and current generated by the machine and the GSC is controlled as per the grid voltages and DC link voltage [9]. The outline structure of PMSG wind farm non-linear backstepping controllers can be observed in figure 2.

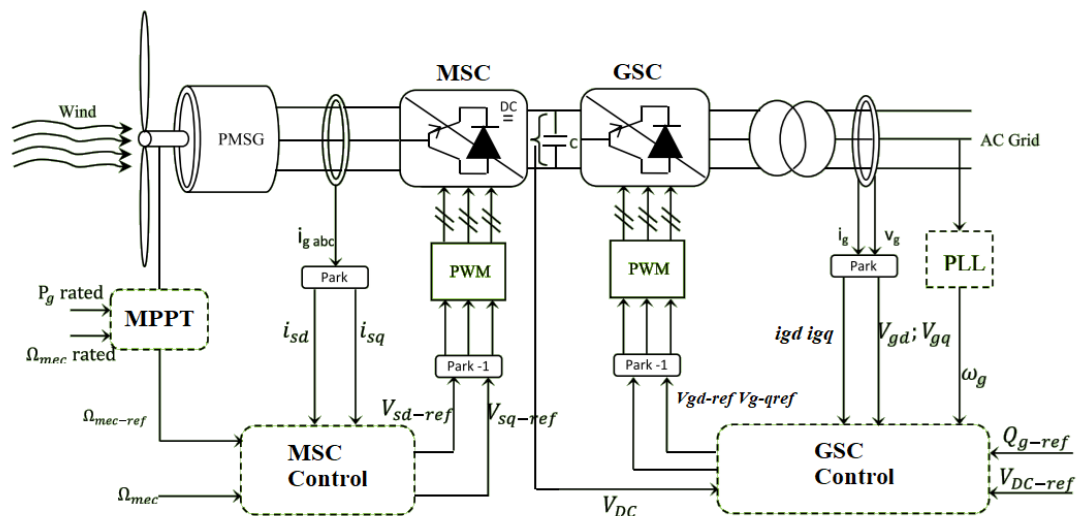


Figure 2: Non-linear Backstepping controller for PMSG

The reference signals for the MSC Sin PWM technique are generated by the stator currents and speed feedback signals from the PMSG [10]. The speed reference signal ( $\Omega_{mec\ ref}$ ) is generated by the MPPT control with feedback from wind speed ( $V_w$ ) and speed controller (PI) [11]. The internal structure of the MPPT control can be observed in figure 3.

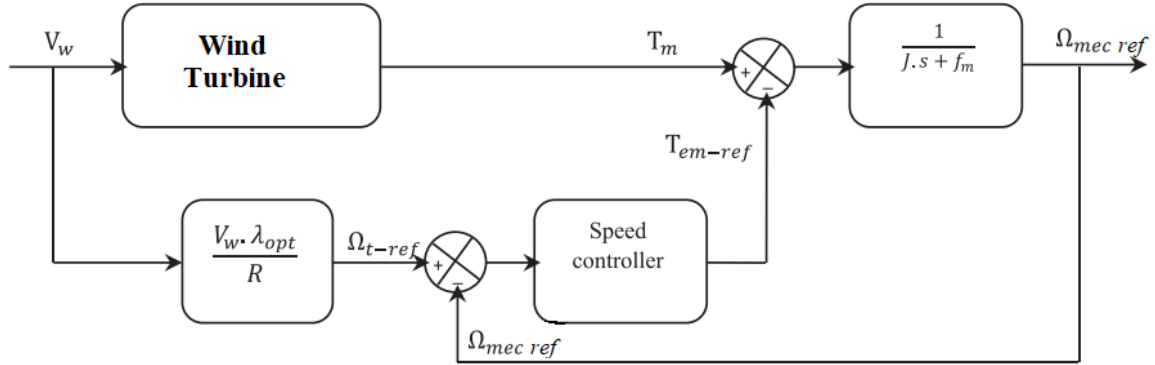


Figure 3: MPPT control structure

The  $\Omega_{mec\ ref}$  signal is generated by the comparison of mechanical torque ( $T_m$ ) and electromagnetic torque ( $T_{em-ref}$ ) which is expressed as:

$$\Omega_{mec\ ref} = (T_m - T_{em-ref}) \left( \frac{1}{J \cdot s + f_m} \right) \quad (1)$$

Here,  $J$  is the inertia and  $f_m$  is the friction constant of PMSG [12]. The  $T_m$  signal is generated by the wind turbine with input  $V_w$  and the  $T_{em-ref}$  is given as:

$$T_{em-ref} = (\Omega_{mec\ ref} - \Omega_{t\ ref}) \left( K_{ps} + \frac{K_{is}}{s} \right) \quad (2)$$

Here,  $K_{ps}$   $K_{is}$  are the speed controller (PI) proportional and integral gains tuned as per the response of the  $\Omega_{mec\ ref}$  to the changes of  $V_w$ . The turbine reference speed ( $\Omega_{t\ ref}$ ) is expressed as:

$$\Omega_{t\ ref} = \frac{V_w \cdot \lambda_{opt}}{R} \quad (3)$$

Here,  $\lambda_{opt}$  is the optimal tip speed ratio of the turbine and  $R$  is the radius of the turbine blades. These values are considered as per the rating of the wind farm. From the  $\Omega_{mec\ ref}$  and  $\Omega_{mec}$  signals the reference signals for the controller are expressed as:

$$V_{sd-ref} = \frac{1}{2} \gamma_{\Omega}^2 \quad (4)$$

Here,  $\gamma_{\Omega} = \Omega_{mec\ ref} - \Omega_{mec}$ , comparison of reference speed and measured speed from PMSG.

$$V_{sq-ref} = \frac{1}{2} (\gamma_{\Omega}^2 + \gamma_d^2 + \gamma_q^2) \quad (5)$$

$$\gamma_d = i_{sd-ref} - i_{sd} \quad (6)$$

$$\gamma_q = i_{sq-ref} - i_{sq} \quad (7)$$

Here,  $i_{sd}$   $i_{sq}$  are the measured dq components of stator current generated by Park's transformation [13]. As active power for the rotor is not considered the  $i_{sd-ref}$  is taken as '0' and the  $i_{sq-ref}$  is given as:

$$i_{sq-ref} = -\frac{T_{em}}{\varphi} \quad (8)$$

Here,  $T_{em}$  is the electromagnetic torque and  $\varphi$  is the flux of the PMSG.

The GSC controlled takes signals from grid which include dq component grid voltages ( $V_{gd}$   $V_{gq}$ ), GSC currents ( $I_{gd}$   $I_{gq}$ ), angular frequency ( $\omega_g$ ), Reactive power reference ( $Q_{g-ref}$ ) and DC link voltage reference ( $V_{dc-ref}$ ). The GSC reference signals are expressed as:

$$V_{gd-ref} = R_g \cdot i_{gd} - L_g \omega_g \cdot i_{gq} - L_g K_{gd} \cdot \gamma_{gd} + V_{gd} \quad (9)$$

$$V_{gq-ref} = R_g \cdot i_{gq} + L_g \omega_g \cdot i_{gd} - L_g K_{gq} \cdot \gamma_{gq} + V_{gq} \quad (10)$$

$$\gamma_{gd} = i_{gd-ref} - i_{gd} \quad (11)$$

$$\gamma_{gq} = i_{gq-ref} - i_{gq} \quad (12)$$

$$i_{gd-ref} = (V_{dc-ref} - V_{dc}) \left( K_{pv} + \frac{K_{iv}}{s} \right) \quad (13)$$

$$i_{gq-ref} = -\frac{Q_{g-ref}}{1.5 V_{gq}} \quad (14)$$

As the  $Q_{g-ref}$  is taken as '0' considering no reactive power exchange,  $i_{gq-ref}$  is calculated to be '0'. Both the reference dq components of the RSC and GSC ( $V_{sd-ref}, V_{sq-ref}$  and  $V_{gd-ref}, V_{gq-ref}$ ) are converted to Sin waveforms using inverse Park's transformation expressed as:

$$\begin{bmatrix} V_{a-ref} \\ V_{b-ref} \\ V_{c-ref} \end{bmatrix} = \begin{bmatrix} \sin(wt) & \cos(wt) \\ \sin\left(wt - \frac{2\pi}{3}\right) & \cos\left(wt - \frac{2\pi}{3}\right) \\ \sin\left(wt + \frac{2\pi}{3}\right) & \cos\left(wt + \frac{2\pi}{3}\right) \end{bmatrix} \quad (15)$$

These reference signals are compared to high frequency triangular carrier waveform generating which generates pulses for the MSC and GSC with respect to the reference signals [14]. For further enchantment of the non-linear backstepping controller, the DC voltage regulator (PI) is replaced with FLC for more DC link voltage stability. The design of FLC for the DC voltage regulator is discussed in next section.

### III. FLC MODELING

The FLC is considered to be an advanced controller with capability of generating fastest nearest value generation. The FLC is a great replacement to many control structures of a closed loop system for faster response of the plant. In the non-linear backstepping controller the DC voltage regulator is updated with FLC which generates the  $i_{gd-ref}$  in the GSC control [15]. The input to the FLC is the error signal produced by comparison of DC link voltage to the reference value. The FLC has three variables which include two input variables error (e), change in error (e-1) and one output variable (o). The FLC structure considered is 'mamdani' generally used for simple fuzzy designs [16]. Each variable has five membership functions modeled in triangular shape. The triangular shape determines the preciseness of the controller with nearest value selection. The figure 4 represents the membership functions of the three variables used in the FLC.

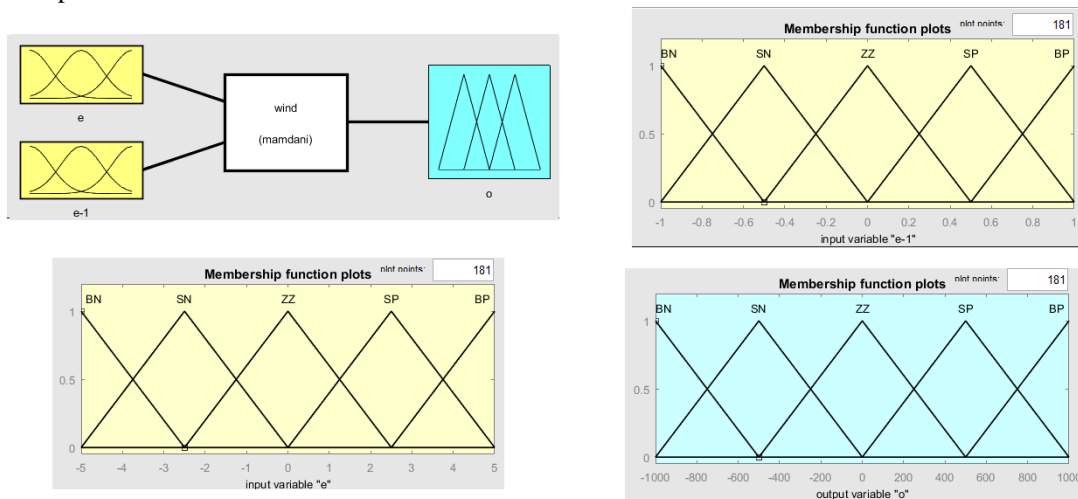


Figure 4: FLC variable structures

Each membership function of the variables are specified with names given as BN (Big Negative), SN (Small Negative), ZZ (Zero), SP (Small Positive), BP (Big Positive). The shapes, names and number of the membership functions are same in each variable with only change is the range [17]. The (e) variable is set with a range between -5 to +5 and (e-1) variable is set in -1 to +1. The FLC is tuned by varying the range of the output variable 'o' which is finalized to -1000 to +1000. The output of the FLC is generated by a 25-rule base set as per the signal value in that particular membership function range [18]. The 25-rule base for the FLC is given in table 1.

Table 1: 25-rule base for FLC

Rule base		'e'				
		PB	PS	ZZ	NS	NB
e-1	NB	PS	PB	NB	ZZ	NS
	NS	PB	PS	ZZ	NS	NB
	ZZ	ZZ	ZZ	ZZ	ZZ	ZZ
	PS	PB	PS	ZZ	NS	NB
	PB	PB	ZZ	ZZ	NB	NS

As per the given membership functions and rule table 1 the FLC is modeled and integrated into the non-linear backstepping controller [19]. The figure 5 represents the FLC modeling for the DC voltage regulator in GSC control.

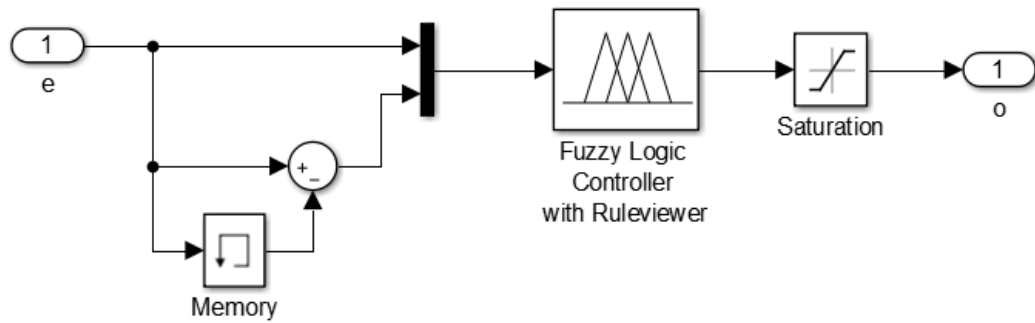


Figure 5: FLC modeling

In the given modeling the ‘memory’ block creates delay to the signal and generates previous value. The comparison of present and previous value determines the change in error signal (e-1). Both the signals are given input to the ‘Fuzzy Logic Controller with Ruleviewer’ block which generates the output signal ‘o’. A ‘saturation’ block is used to limit the output value in specific range for stability of the system [20]. The rule viewer with respect to the input signal values is shown in figure 6.

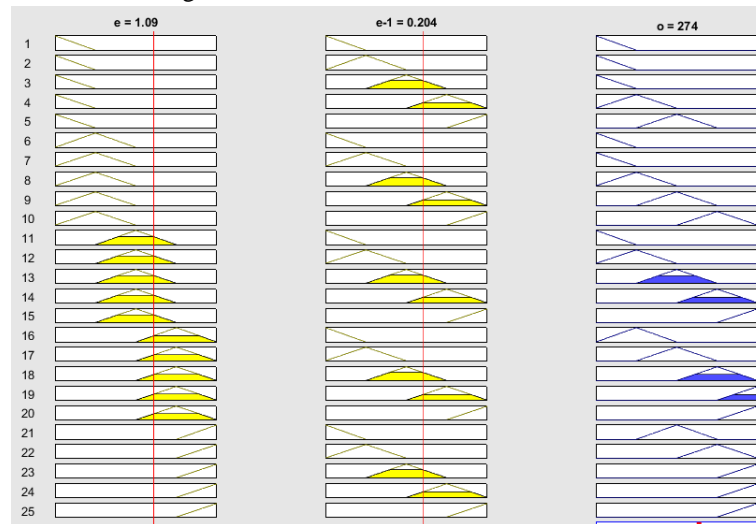


Figure 6: Rule viewer of the FLC design

The proposed FLC design is integrated into the GSC and a comparative analysis is done with conventional PI controller in the next section.

#### IV. SIMULATION RESULT ANALYSIS

The complete system with PMSG connected to back-to-back VSCs and the GSC MSC controller are modelled using ‘Powersystems’ blocks in Simulink environment of MATLAB software. The non-linear backstepping controller is modelled using commonly used blocks and control blocks. The DC voltage regulator FLC is designed using the ‘Fuzzy’ tool of the software defining the membership functions and rule base. The parameters to the blocks are given as per the configuration table 2 for a 2MG wind farm.

Table 2: Configuration parameters of test system

Name of the module	Parameter values
Grid	11kV 50Hz 100MVA Step down T/F = 11kV/1.5kV, 50Hz, 2.5MVA
PMSG	$P_n = 2\text{MW}$ , $V_n = 1.5\text{kV}$ , $R_s = 0.0304$ , $L_d = L_q = 1.8\text{mH}$ , flux = 4.633, $J = 300000$ , $N_p = 75$ , $w_{\text{rated}} = 4.1888$ , $R_f = 0.0034\Omega$ , $L_f = 0.0011\text{H}$ , $C_f = 120\text{kVAR}$ .

Wind turbine	$P_n = 2\text{MW}$ , Base wind speed = 10m/s, Maximum power at base wind speed = 1pu, Base rotation speed = 1.2pu.
RSC	$R_{igbt} = 1\text{m}\Omega$ , $K_{pi} = 0.1361$ , $K_{ii} = 2.7221$ , $i_{d\text{ref}} = 0$ , $f_s = 1350\text{Hz}$ .
GSC	$R_{igbt} = 1\text{m}\Omega$ , $K_{pv} = 8$ , $K_{iv} = 400$ , $K_{pg} = 0.83$ , $K_{ig} = 5$ , $f_s = 2250\text{Hz}$ .

The system has been updated and simulations have been run for different wind speeds to analyze the performance of the wind farm. Various parameters such as power, voltage and machine variables have been plotted with time as a reference. The simulation time taken is 30 seconds, with variable wind speeds given as 8 m/s from 0 s to 10 s, 11 m/s from 10 s to 20 s, and 9 m/s from 20 s to 30 s. All the graphs have been plotted with a comparative analysis of PI and FLC in the GSC controller.

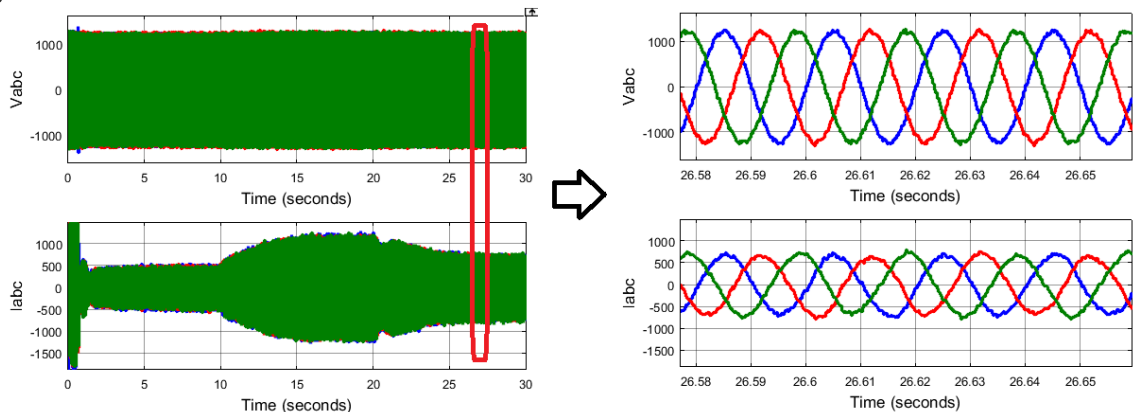


Figure 7: PMSG wind farm voltage and currents

The figure 7 represents the 3-ph voltages and currents of the PMSG. The 3-ph voltage are always constant from initial simulation time with phase peak value of 1225V ( $1500\text{Vrms} * \sqrt{2}/\sqrt{3}$ ). The current varies as per the change in wind speed, creating change in power generated by the PMSG.

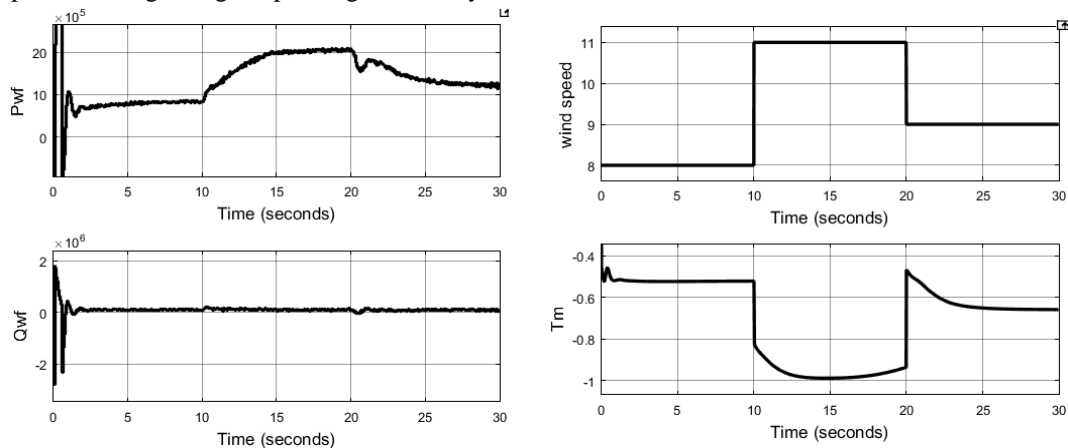


Figure 8: Active power (Pwf), Reactive power (Qwf), wind speed (Vw) and mechanical torque (Tm) of the PMSG wind farm

In the figure 8 the total power generated by the PMSG wind farm as per the wind speeds can be observed. The active power is noted to be 0.9MW during the period 0-10s, raising to 2MW during 10-20s period and drops to 11MW during 20-30s duration. This is caused by the wind speed changes which varies the mechanical torque (Tm). The negative value of Tm represents generator operating condition in Simulink software. The Tm raises to 1pu during the period 10-20s as maximum wind speed is given. In any given condition the reactive power exchange is maintained zero throughout the simulation.

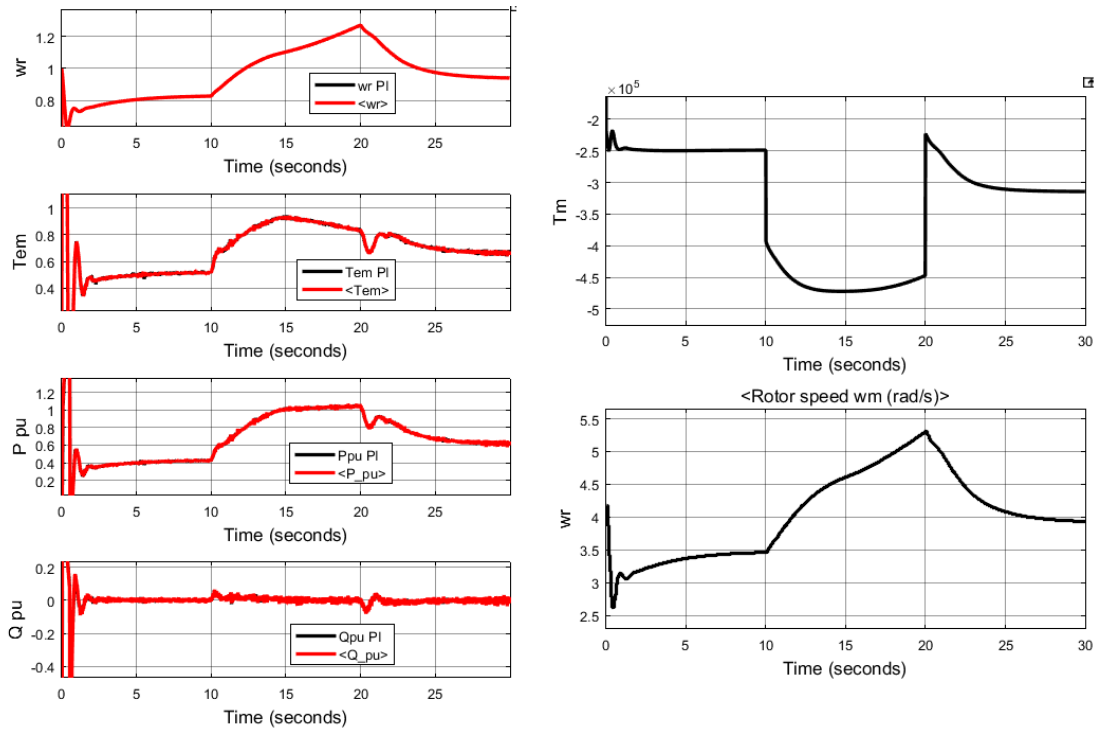


Figure 9: mechanical parameters of PMSG

As per the changes in the wind speed the figure 9 shows the parameters comparison of PMSG with PI and FLC in GSC. All the parameters are compared in perunit representation for comparison. It is observed that there are not change in the values of the PMSG outputs for change in the controller. The rotor speed varies between 3rad/s to 5.5rad/s as per the wind speeds.

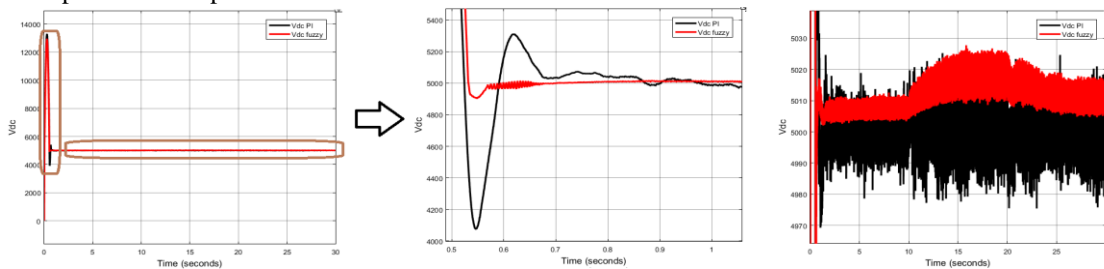


Figure 10: DC link voltage comparison

The figure 10 has the DC link voltage comparison between PI and FLC in the GSC. There is no much improvement in peak value but there is a drop in settling time of the voltage from 0.8s to 0.5s. The ripple in the DC link voltage is also reduced for which improves the THD of the voltage and current signals of the wind farm. The THDs of the phase A voltage and current are determined using FFT analysis tool from Simulink and are presented in figure 11 and 12.

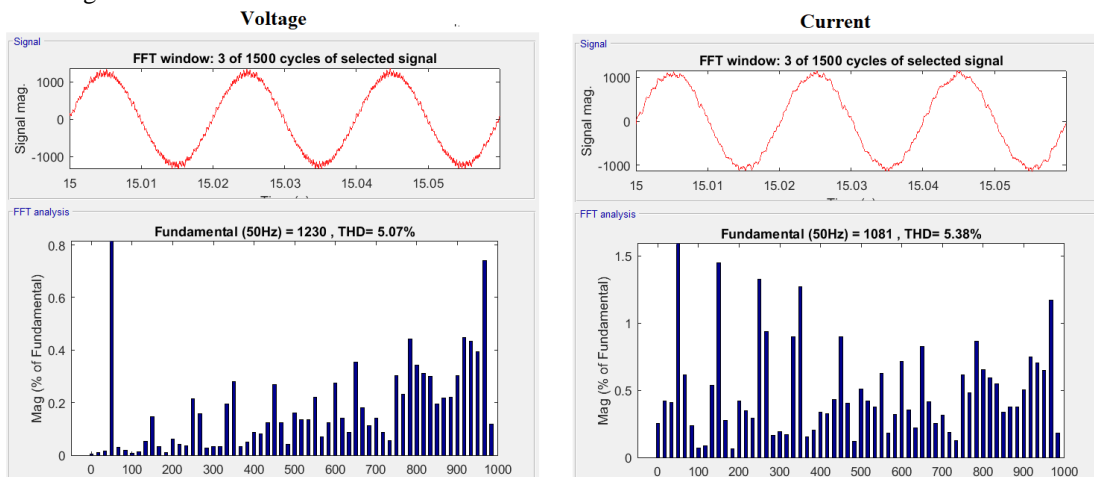


Figure 11: THDs of PMSG voltage and current with PI controller in GSC

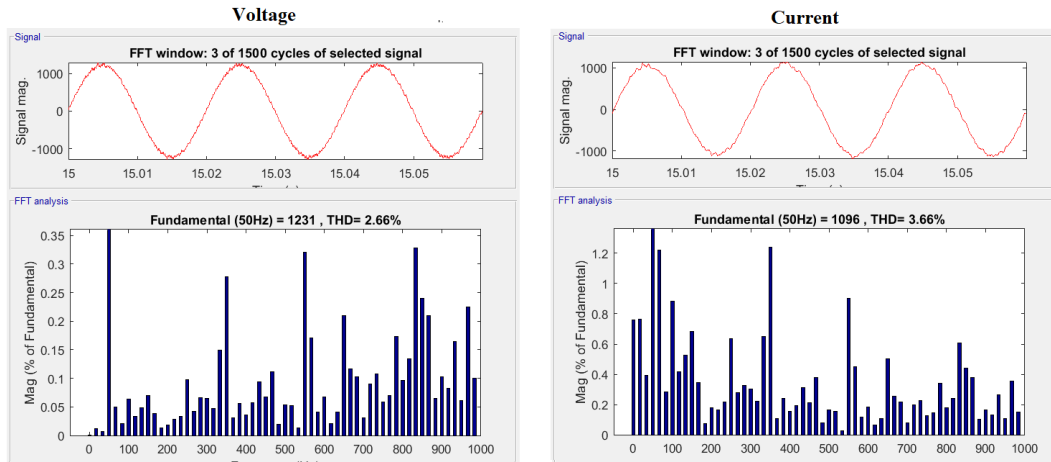


Figure 12: THDs of PMSG voltage and current with FLC in GSC

As per figure 11 and 12 the THD of the voltage is dropped from 5.07% to 2.66% and current is dropped from 5.38% to 3.66%. This drop is caused by the FLC integration into the GSC non-linear backstepping controller. A comparison table 3 is given with comparison of different parameters of the wind farm to determine the better performing controller.

Table 3: Parametric comparison table

Name of the parameter	PI	FIS
Vdc ripple	1%	0.5%
Vdc settling time	0.5s	0.8s
THD of V	5.07%	2.66%
THD of I	5.38%	3.66%

### V. CONCLUSION

This paper presents the design and simulation of a 2MW PMSG wind farm operated by a novel non-linear backstepping controller. The wind farm is considered standalone and can generate power even during grid islanding conditions. However, in the modeling, the grid is considered for power sharing from the wind farm. The PMSG is a fragile machine with more disturbances for the wind changes. The machine's speed varies drastically based on wind speeds that vary voltages and powers of the wind farm rapidly. To achieve stability in the parameters, a non-linear backstepping controller is adopted and further modified with FLC design. A comparative analysis between the conventional PI and FLC is presented with different parameters. It is observed that the ripple and settling time of DC link voltage are reduced by nearly half. There is also an improvement in the THDs of the voltage and current of the wind farm, reducing half of the previous controller value. The power output of the wind farm remains the same with no significant changes and varies according to the wind speed given. From the comparison table, it is validated that the FLC integrated system is more stable and has reduced harmonic content in the signals.

### REFERENCES

- [1] A. Qazi *et al.*, "Towards Sustainable Energy: A Systematic Review of Renewable Energy Sources, Technologies, and Public Opinions," in *IEEE Access*, vol. 7, pp. 63837-63851, 2019, doi: 10.1109/ACCESS.2019.2906402.
- [2] U. k. Nath and R. Sen, "A Comparative Review on Renewable Energy Application, Difficulties and Future Prospect," *2021 Innovations in Energy Management and Renewable Resources(52042)*, Kolkata, India, 2021, pp. 1-5, doi: 10.1109/IEMRE52042.2021.9386520.
- [3] M. Zou, Y. Wang, C. Zhao, J. Xu, X. Guo and X. Sun, "Integrated Equivalent Model of Permanent Magnet Synchronous Generator Based Wind Turbine for Large-scale Offshore Wind Farm Simulation," in *Journal of Modern Power Systems and Clean Energy*, vol. 11, no. 5, pp. 1415-1426, September 2023, doi: 10.35833/MPCE.2022.000495.
- [4] W. Du, W. Dong and H. F. Wang, "Small-Signal Stability Limit of a Grid-Connected PMSG Wind Farm Dominated by the Dynamics of PLLs," in *IEEE Transactions on Power Systems*, vol. 35, no. 3, pp. 2093-2107, May 2020, doi: 10.1109/TPWRS.2019.2946647.

- [5] Feng Guo, Jie Yu, Qiulong Ni, Zhiyi Zhang, Jianhui Meng, Yi Wang, "Grid-forming control strategy for PMSG wind turbines connected to the low-frequency AC transmission system", *Energy Reports*, Volume 9, 2023, Pages 1464-1472, ISSN 2352-4847, <https://doi.org/10.1016/j.egy.2022.12.083>.
- [6] El Mourabit, Youness, Aziz Derouich, Abdelaziz El Ghzizal, Najib El Ouanjli and Othmane Zamzoum. "Nonlinear backstepping control for PMSG wind turbine used on the real wind profile of the Dakhla-Morocco city." *International Transactions on Electrical Energy Systems* 30 (2020).
- [7] Agarwal, Nirmal & Prateek, Manish & Saxena, Abhinav & Singh, Gyanendra. (2023). A Novel Design of Hybrid Fuzzy Poisson Fractional Order Proportional Integral Derivative Controller for the Wind Driven Permanent Magnet Synchronous Generator. *IEEE Access*. PP. 1-1. 10.1109/ACCESS.2023.3329941.
- [8] Salime, H.; Bossoufi, B.; El Mourabit, Y.; Motahhir, S. Robust Nonlinear Adaptive Control for Power Quality Enhancement of PMSG Wind Turbine: Experimental Control Validation. *Sustainability* **2023**, *15*, 939. <https://doi.org/10.3390/su15020939>
- [9] S. Zhang, E. -M. Yong, Y. Zhou and W. -Q. Qian, "Dynamic backstepping control for pure-feedback non-linear systems," in *IMA Journal of Mathematical Control and Information*, vol. 37, no. 1, pp. 670-693, March 2020, doi: 10.1093/imamci/dnz019.
- [10] E. M. Youness, D. Aziz, E. G. Abdelaziz, Z. Othmane and E. O. Najib, "Nonlinear Backstepping Control of Variable Speed Wind Turbine Based on Permanent Magnet Synchronous Generator," *2019 International Conference on Wireless Technologies, Embedded and Intelligent Systems (WITS)*, Fez, Morocco, 2019, pp. 1-7, doi: 10.1109/WITS.2019.8723798.
- [11] El Mourabit Youness, Derouich Aziz, El Ghzizal Abdelaziz, Bouchnaif Jamal, El Ouanjli Najib, Zamzoum Othmane, Mezioui Khalid, Badre BOSSOUFI, "Implementation and validation of backstepping control for PMSG wind turbine using dSPACE controller board, *Energy Reports*", Volume 5, 2019, Pages 807-821, ISSN 2352-4847, <https://doi.org/10.1016/j.egy.2019.06.015>.
- [12] Boudali, A., Negadi, K., Bouradi, S., Berkani, A., Marignetti, F. (2021). Design of nonlinear backstepping control strategy of PMSG for hydropower plant power generation. *Journal Européen des Systèmes Automatisés*, Vol. 54, No. 1, pp. 1-8. <https://doi.org/10.18280/jesa.540101>
- [13] E. Mahersi and A. Kheder, "Adaptive backstepping control applied to wind PMSG system," *2016 7th International Renewable Energy Congress (IREC)*, Hammamet, Tunisia, 2016, pp. 1-6, doi: 10.1109/IREC.2016.7478910.
- [14] Ayadi, M., Derbel, N. Nonlinear adaptive backstepping control for variable-speed wind energy conversion system-based permanent magnet synchronous generator. *Int J Adv Manuf Technol* **92**, 39-46 (2017). <https://doi.org/10.1007/s00170-017-0098-3>
- [15] Abdel Ghani Aissaoui, Ahmed Tahour, Mohamed Abid, Najib Essounbouli, Frederic Nollet, "Power Control of Wind Turbine based on Fuzzy Controllers", *Energy Procedia*, Volume 42, 2013, Pages 163-172, ISSN 1876-6102, <https://doi.org/10.1016/j.egypro.2013.11.016>.
- [16] Salem, Ahmed & Nouraldin, Noura & Azmy, Ahmed & Abdellatif, Walid. (2019). A Fuzzy Logic-Based MPPT Technique for PMSG Wind Generation System. 9.
- [17] Rosyadi, M.; Muyeen, S.M.; Takahashi, R.; Tamura, J. A Design Fuzzy Logic Controller for a Permanent Magnet Wind Generator to Enhance the Dynamic Stability of Wind Farms. *Appl. Sci.* 2012, *2*, 780-800. <https://doi.org/10.3390/app2040780>
- [18] Jaiswal A, Belkhier Y, Chandra S, Priyadarshi A, Bajaj M, Pushkarna M, Elgamli E, Shouran M and Kamel S (2022) Design and implementation of energy reshaping based fuzzy logic control for optimal power extraction of PMSG wind energy converter. *Front. Energy Res.* 10:966975. doi: 10.3389/fenrg.2022.966975
- [19] Toumi, Ilham & Meghni, Billel & Djamel, Taibi. (2022). Control for PMSG wind energy conversion system based on Adaptive Fuzzy Logic Controller. 1-7. 10.1109/ICPEA51060.2022.9791215.
- [20] Mhamed Fannakh, Mohamed Larbi Elhafyani, Smail Zouggar, Hassan Zahboune "Overall fuzzy logic control strategy of direct driven PMSG wind turbine connected to grid" *International Journal of Electrical and Computer Engineering (IJECE)* p-ISSN 2088-8708, e-ISSN 2722-2578, Vol 11, No 6, December 2021. doi: <http://doi.org/10.11591/ijece.v11i6.pp5515-5529>